Thermochimica Acta, 223 (1993) 145–156
Elsevier Science Publishers B.V., Amsterdam

The phase diagrams of $LiNO_3$–$NaNO_3$ and $LiNO_3$–KNO_3: the behaviour of liquid mixtures

M.J. Maeso [a] and J. Largo *,[b]

[a] *Departamento de Física Aplicada, Universidad de Cantabria, 39005 Santander (Spain)*
[b] *Departamento de Ingeniería Eléctrica y Energética, Universidad de Cantabria, 39005 Santander (Spain)*

(Received 11 December 1992; accepted 13 January 1993)

Abstract

The binary phase diagrams of $LiNO_3$–$NaNO_3$ and $LiNO_3$–KNO_3 are studied by means of differential scanning calorimetry (DSC). For each phase diagram, the temperatures for solids and liquids have been determined and tabulated. Two models, based on regular solution theory, are employed to reproduce the phase diagrams. The first uses the values of the temperatures and enthalpies of fusion of the nitrates and the change in the heat capacity on melting, all of which are determined by differential scanning calorimetry. In the second model, we assume a variation of interaction energy with temperature to preserve regular solution treatment for the mixtures of alkaline nitrates.

INTRODUCTION

Alkaline nitrates are important and inexpensive industrial chemical substances with applications in many fields and technologies. Some of their mixtures also show interesting properties, such as low melting temperatures. Furthermore, they are chemically stable and non-corrosive for many common structural materials up to about 650 K.

An increasing number of calculations have been performed to predict phase diagrams [1, 2]. Such calculations often provide information about the thermodynamic properties of these materials accurate enough to avoid tedious and difficult experiments. In the present work, we determine by differential scanning calorimetry the phase diagrams of $LiNO_3$–$NaNO_3$ and $LiNO_3$–KNO_3. Experimenal results are compared with the predictions of two models based on regular solutions theory.

* Corresponding author.

EXPERIMENTAL

A Perkin-Elmer differential scanning calorimeter (DSC-2) was used for all measurements. The DSC was calibrated with Perkin-Elmer standards samples In and K_2CrO_4 for temperature and energy, and sapphire for heat capacity.

All our samples consisted of reagent grade lithium nitrite, sodium nitrate and potassium nitrate, kept at 380 K under vacuum for 24 h. Samples were prepared at 10% mole intervals and ground in a micromill to ensure uniformity. Small samples (<15 mg) were encapsuled in hermetically sealed aluminium pans.

At least three successive runs were carried out for each sample. Generally, the results of the third run were in agreement with those of the second run (indicating equilibrium conditions) and only such data are reported here. An optimal reproducibility and well-pronounced peaks were obtained with heating and cooling rates of $10\,K\,min^{-1}$. Different DSC profiles of the salt mixtures were obtained using heating rates from 1.25 to $20\,K\,min^{-1}$, sample sizes of 1–20 mg, sample pre-treatment (prior grinding or fusion), and DSC energy scales from 0.5 to 5 mcal sec^{-1}.

The lowest and highest temperatures at which the DSC traces for the melting of the salt samples deviated from a straight baseline were consistent from run to run and sample to sample. Therefore, the initial and final points of deviation from the baseline were chosen as the solid and liquid temperatures for the samples. These are given in Tables 1 and 2 for the systems $LiNO_3$–$NaNO_3$ and $LiNO_3$–KNO_3, respectively.

The liquid curve, established by cooling the melts after they were held at about 20 K above their melting point for at least 5 min, showed small differences when compared to that obtained by melting, in the order of 3–4 K. We attribute these small differences to undercooling effects. Therefore, we have corrected all measured data for liquid and solid phases obtained from cooling runs in the temperature range 480–610 K, by adding $\Delta T = +3$ K.

The experimentally determined liquid curves for the systems $LiNO_3$–$NaNO_3$ and $LiNO_3$–KNO_3 are in good agreement with previous measurements [3, 4], but the solid line is much flatter than was previously reported, as occurs for the system $NaNO_3$–KNO_3. We assume, in accordance with Kramer and Wilson [5], that this flattening does not indicate a eutectic with limited solid solution or contamination of the samples, such as that due to water.

BASIC EQUATIONS

The Gibbs energy of a real mixture is usually given in the form [6]

$$G(P, T, x) = G^{id}(P, T, x) + G^{E}(P, T, x) \quad (1)$$

TABLE 1

Liquid and solid temperatures of the system $LiNO_3$–$NaNO_3$

x_{LiNO_3}	T_L/K	T_S/K
1.00	527.5	527.5
0.95	522.9	500.6
0.90	517.9	487.2
0.85	512.6	474.3
0.80	507.1	474.0
0.75	501.0	474.0
0.70	495.2	474.0
0.65	488.7	474.0
0.60	482.0	474.0
0.55	474.2	474.0
0.50	482.5	474.0
0.45	490.7	474.0
0.40	499.4	474.0
0.35	509.7	474.0
0.30	520.1	474.0
0.25	529.3	474.0
0.20	538.7	474.0
0.15	547.8	495.3
0.10	558.7	520.2
0.05	569.1	550.6
0.00	579.1	579.1

where x is the mole fraction of the second component 2. The second member is the sum of two terms: the first gives the ideal contribution and the second the deviation from ideal mixing behaviour, the excess Gibbs energy. It is obvious that the deviation from ideal mixing behaviour is zero for pure components. This implies that G^E should be represented by a mathematical expression in which this condition is fulfilled implicitly. One of the most frequently used forms is the Redlich–Kister [7]

$$G^E = x(1-x)\sum_i A_i(1-2x)^{i-1} \qquad i = 1, 2, \ldots \tag{2}$$

A standard ideal mixture is characterized by the condition that total dissociation exists in the melt which is an ideal mixture with respect to the individual species, and that no complex ions are found. Deviations from the standard ideal mixture are given by the activity coefficients for molten salts.

The activity coefficients are defined by

$$RT \ln \gamma_i = \mu_i^{real} - \mu_i^{id} = \mu^E \tag{3}$$

and they are related to G^E by the equation

$$G^E/RT = (1-x)\ln \gamma_1 + x \ln \gamma_2 \tag{4}$$

TABLE 2

Liquid and solid temperatures of the system $LiNO_3$–KNO_3

x_{KNO_3}	T_L/K	T_S/K
1.00	527.5	527.5
0.95	521.9	482.2
0.90	514.3	447.1
0.85	506.2	412.3
0.80	497.7	410.0
0.75	488.8	410.0
0.70	477.9	410.0
0.65	466.5	410.0
0.60	453.6	410.0
0.55	440.1	410.0
0.50	427.2	410.0
0.45	410.2	410.0
0.40	437.6	410.0
0.35	446.0	410.0
0.30	476.0	410.0
0.25	504.2	410.0
0.20	524.4	432.3
0.15	552.6	463.5
0.10	572.8	517.3
0.05	590.4	552.1
0.00	612.2	612.2

We shall use as a general expression for G^E the series [8]

$$G^E = x(1-x)(a' + b'x + c'x^2 + \ldots) \tag{5}$$

to fit the experimental results, and it will be sufficient for our purposes to retain only the first three terms. For the activity coefficients, we then obtain

$$\left.\begin{aligned} \mu_1^E &= RT \ln \gamma_1 = A_2x^2 + A_3x^3 + A_4x^4 \\ \mu_2^E &= RT \ln \gamma_2 = B_2(1-x)^2 + B_3(1-x)^3 + B_4(1-x)^4 \end{aligned}\right\} \tag{6}$$

We shall consider the special cases of regular mixtures, which can be obtained from the preceding expressions by introducing $A_3 = A_4 = \ldots = B_3 = B_4 = \ldots = 0$. Then we obtain

$$\left.\begin{aligned} G^E/RT &= Wx(1-x) \\ \ln \gamma_1 &= Wx^2 \\ \ln \gamma_2 &= W(1-x)^2 \end{aligned}\right\} \tag{7}$$

The melting behaviour of a eutectic system of only two components is commonly described by thermodynamic relations in the region of solid–liquid equilibrium. For an ideal mixture of non-electrolytes, such a

description, at isobaric conditions, is given in the form

$$\ln a_1 = \frac{\Delta H_1^*}{R}\left[\frac{1}{T_{f,1}} - \frac{1}{T_L}\right] + \frac{\Delta C_p}{R}\left[\frac{T_{f,1}}{T_L} - 1 - \ln\frac{T_{f,1}}{T_L}\right] \quad (8)$$

where a_1 is the activity of the solvent at the liquid temperature T_L with respect to pure supercooled liquid solvent at the reference state, ΔH_1^* is the heat of fusion of the pure component at the melting point, T_L is the equilibrium temperature, and ΔC_p is the difference between the molar heat capacities at constant pressure of pure component 1 for the liquid and solid phases

$$\Delta H(T) = \Delta H(T_{f,1}) + \int \Delta C_p \, dT \quad (9)$$

In the case of sodium and potassium nitrates, it is necessary to consider the contribution due to the solid–solid transition in the liquid line equations for $T_L < T_{tr}$

$$\frac{\Delta H_{tr}}{R}\left[\frac{1}{T_{tr}} - \frac{1}{T_L}\right] \quad (10)$$

Assuming the usual form, $a = \gamma x$, for the activity of a mixture of monovalent salts having a common ion [3], eqn. (8) enables us to construct the isobaric melting line for binary systems with regular behaviour, on the basis of the properties of the main components alone. In fact, it is an empirical statement that each branch of the liquid curve may be reconstructed by means of a single parameter W in the form

$$T_L = \frac{\Delta H^* + Wx^2}{(\Delta H^*/T_{f,1}) - R\ln(1-x)} \quad (11)$$

We can obtain this parameter for regular solutions from the slope of the curve in the plot of activity coefficients, as given by eqn. (7), as a function of x^2.

RESULTS AND DISCUSSION

The activity coefficients of $LiNO_3$, $NaNO_3$ and KNO_3 in the binary systems $LiNO_3$–$NaNO_3$ and $LiNO_3$–KNO_3 may be obtained by a combination of the calorimetric data of the nitrates obtained from DSC [9], see Table 3, and the cryoscopic data for the two systems given in Tables 1 and 2.

The results for the binary systems $LiNO_3$–$NaNO_3$ and $LiNO_3$–KNO_3 are given in Tables 4 and 5. The corresponding excess thermodynamic

TABLE 3

Thermodynamic properties of the pure salts ($LiNO_3$, $NaNO_3$ and $NaNO_3$)

Salt	T_{tr}/K	ΔH_{tr}/kJ mol^{-1}	T_f/K	ΔH_f/kJ mol^{-1}	ΔC_p/J mol^{-1}
$LiNO_3$	–	–	527.5	24.5	18.5
$NaNO_3$	540.1	3.68	579.1	14.7	12.6
KNO_3	405.6	5.7	612.2	10.0	0.3

potentials are given by the expressions

$$\left.\begin{aligned} RT_L \ln \gamma_{LiNO_3} &= -5.06 - 280.25x^2 \quad 0.55 \le (1-x) \le 1.0 \\ RT_L \ln \gamma_{NaNO_3} &= -2.51 - 205.74(1-x)^2 \quad 0.65 \le x \le 1.0 \end{aligned}\right\} \quad (12)$$

$$\left.\begin{aligned} RT_L \ln \gamma_{LiNO_3} &= -12.53 - 2087.3x^2 \quad 0.65 \le (1-x) \le 1.0 \\ RT_L \ln \gamma_{KNO_3} &= -9.19 - 2075.7(1-x)^2 \quad 0.65 \le x \le 1.0 \end{aligned}\right\} \quad (13)$$

Figures 1 and 2 show the calculated liquid curves of the systems $LiNO_3$–$NaNO_3$ and $LiNO_3$–KNO_3, respectively, obtained by substituting expressions (12) and (13) in eqn. (11), together with the experimental liquid temperatures.

TABLE 4

Activity and activity coefficients for $LiNO_3$ and $NaNO_3$ in the liquid mixture (Li–Na)NO_3

x_{LiNO_3}	T_L/K	a_{LiNO_3}	ln γ_{LiNO_3}
0.95	522.9	0.948 ± 0.003	−0.002
0.90	517.9	0.895 ± 0.004	−0.006
0.85	512.6	0.840 ± 0.005	−0.012
0.80	507.1	0.785 ± 0.005	−0.018
0.75	501.0	0.729 ± 0.006	−0.028
0.70	495.2	0.678 ± 0.007	−0.032
0.65	488.7	0.624 ± 0.007	−0.041
0.60	482.0	0.571 ± 0.008	−0.048
x_{NaNO_3}	T_L/K	a_{NaNO_3}	ln γ_{NaNO_3}
0.95	569.1	0.948 ± 0.002	−0.002
0.90	558.7	0.895 ± 0.005	−0.005
0.85	547.8	0.842 ± 0.005	−0.010
0.80	538.7	0.791 ± 0.005	−0.011
0.75	529.3	0.737 ± 0.006	−0.018
0.70	520.1	0.686 ± 0.007	−0.021
0.65	509.7	0.632 ± 0.007	−0.029
0.60	499.4	0.580 ± 0.008	−0.034

TABLE 5

Activity and activity coefficients for $LiNO_3$ and KNO_3 in the liquid mixture (Li–K)NO_3

x_{LiNO_3}	T_L/K	a_{LiNO_3}	ln γ_{LiNO_3}
0.95	521.9	0.942 ± 0.003	−0.008
0.90	514.3	0.896 ± 0.005	−0.004
0.85	506.2	0.792 ± 0.006	−0.071
0.80	497.7	0.718 ± 0.007	−0.107
0.75	488.8	0.647 ± 0.008	−0.148
0.70	477.9	0.566 ± 0.009	−0.212
0.65	466.5	0.490 ± 0.009	−0.282
0.60	453.6	0.413 ± 0.009	−0.373
0.55	440.1	0.343 ± 0.009	−0.473
x_{KNO_3}	T_L/K	a_{KNO_3}	ln γ_{KNO_3}
0.95	590.4	0.9298 ± 0.0011	−0.022
0.90	572.8	0.873 ± 0.002	−0.030
0.85	552.6	0.808 ± 0.004	−0.050
0.80	529.4	0.735 ± 0.005	−0.085
0.75	504.2	0.656 ± 0.007	−0.134
0.70	476.0	0.570 ± 0.008	−0.206
0.65	446.0	0.481 ± 0.009	−0.302

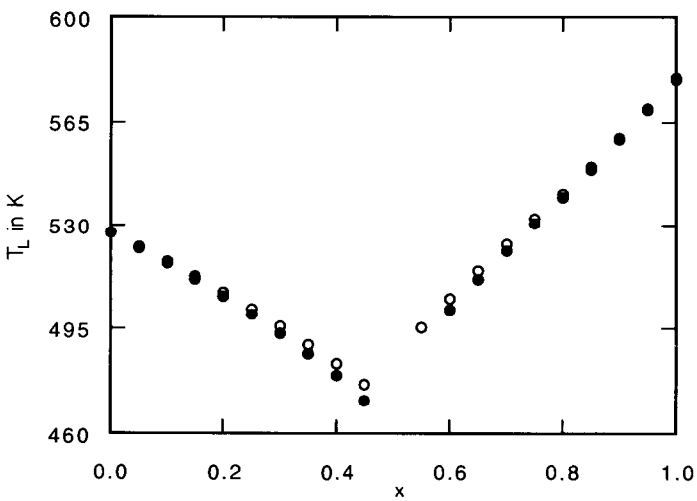

Fig. 1. Liquid temperatures of the system $LiNO_3$–$NaNO_3$ plotted against the mole fraction of $NaNO_3$: ○, experimental values; ●, values of expressions (12).

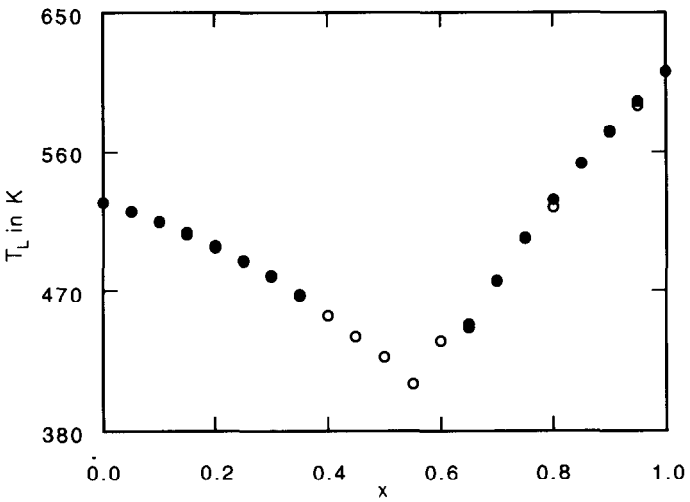

Fig. 2. Liquid temperatures of the system $LiNO_3$–KNO_3 plotted against the mole fraction of KNO_3: ○, experimental values; ●, values of expressions (13).

The results of the present work allow us to conclude that it is possible to reproduce the liquid line of the phase diagrams of $LiNO_3$–$NaNO_3$ and $LiNO_3$–KNO_3. Moreover the use of a single equation for the activity coefficients (7) allows us to obtain, with notable precision, the values of the activity coefficients corresponding to compositions of the liquid line, especially for the $LiNO_3$–KNO_3 system.

Activities for compositions beyond the eutectic may be calculated by analytical integration of the classical Gibbs–Duhem equation. The results of these calculations are given in Tables 6 and 7, respectively.

From the plot of $G^E/RT[x(1-x)]$ as a function of the mole fraction x, it

TABLE 6

Activity coefficients for $LiNO_3$ and $NaNO_3$ in the liquid mixture (Li–Na)NO_3 at compositions beyond the eutectic

x	$\ln \gamma_{LiNO_3}$	$\ln \gamma_{NaNO_3}$
0.40		−0.174
0.35	−0.053	−0.191
0.30	−0.049	−0.210
0.25	−0.044	−0.231
0.20	−0.038	−0.255
0.15	−0.032	−0.285
0.10	−0.023	−0.321
0.05		
0	−0.2620	−0.3644

TABLE 7

Activity coefficients for $LiNO_3$ and KNO_3 in the liquid mixture (Li–K)NO_3 at compositions beyond the eutectic

x	$\ln \gamma_{LiNO_3}$	$\ln \gamma_{KNO_3}$
0.35		−0.302
0.30	−0.833	−0.206
0.25	−1.020	−0.134
0.20	−1.187	−0.085
0.15	−1.337	−0.050
0.10	−1.483	−0.030
0.05	−1.674	−0.022
0.00	−1.958	−2.645

is evident that data fall on a straight line given by

$$G^E/[RTx(1-x)] = A_{12}(1-x) + A_{21}x \tag{14}$$

with $A_{12} = \ln \gamma_1^\infty$ and $A_{21} = \ln \gamma_2^\infty$. From this, we can derive the activity coefficients and the expressions of Margules. The results for liquid mixtures of $LiNO_3$–$NaNO_3$ and $LiNO_3$–KNO_3 are respectively

$$\left.\begin{aligned} \frac{G^E}{RT} &= x(1-x)[-0.452(1-x) - 0.272x] \\ \ln \gamma_{LiNO_3} &= x^2[-0.272 - 0.359(1-x)] \\ \ln \gamma_{NaNO_3} &= (1-x)^2[-0.452 + 0.359x] \end{aligned}\right\} \tag{15}$$

and

$$\left.\begin{aligned} \frac{G^{exc}}{RT_L} &= x(1-x)[-2.356(1-x) - 1.107x] \\ \ln \gamma_{LiNO_3} &= x^2[-1.802 - 1.107(1-x)] \\ \ln \gamma_{KNO_3} &= (1-x)^2[-2.356 + 1.107x] \end{aligned}\right\} \tag{16}$$

The results from these expressions are represented in Figs. 3 and 4 together with values obtained for the experimental activity coefficients. The satisfactory agreement between theory and experiment confirms the validity of this adjustment for liquid mixtures outside the eutectic composition.

The treatment of regular solutions when the excess Gibbs energy calculated from the liquid curve differs from the excess enthalpy is

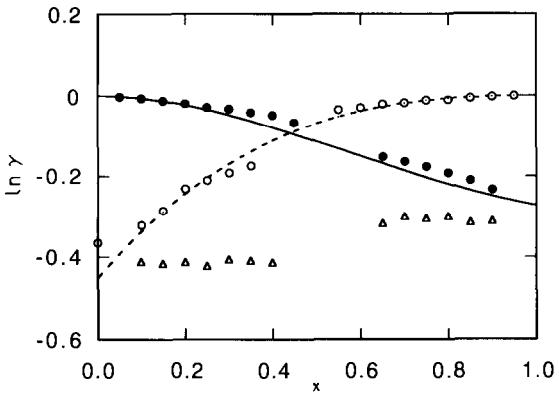

Fig. 3. Experimental activity coefficients (●, values of $LiNO_3$; ○, values of $NaNO_3$) plotted against the mole fraction of $NaNO_3$ in the $LiNO_3$–$NaNO_3$ system solid line, the second of expressions (15); broken line, the third of expressions (15); △, experimental values of $G^E/RTx(1-x)$.

preserved if the deviation is due to a variation in W with temperature. The excess energy is

$$G^E = W(T)x(1-x) \tag{17}$$

and, if it is assumed that for nitrate mixtures a linear variation with temperature for H^E holds [4], we obtain

$$G^E = (a + bT \ln T + cT)x(1-x) \tag{18}$$

The corresponding expressions for the systems $LiNO_3$–$NaNO_3$ and $LiNO_3$–KNO_3 in J mol^{-1}, with values of H^E at 345°C from Kleppa and

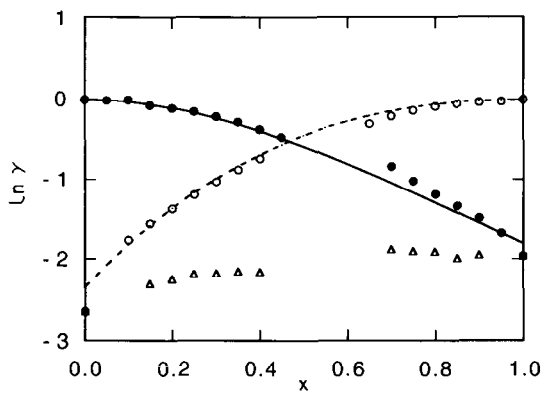

Fig. 4. Experimental activity coefficients (●, values of $LiNO_3$; ○, values of KNO_3) plotted against the mole fraction of KNO_3 in the $LiNO_3$–KNO_3 system. Solid line, the second of expressions (16); broken line, the third of expressions (16); △, experimental values of $G^E/RTx(1-x)$.

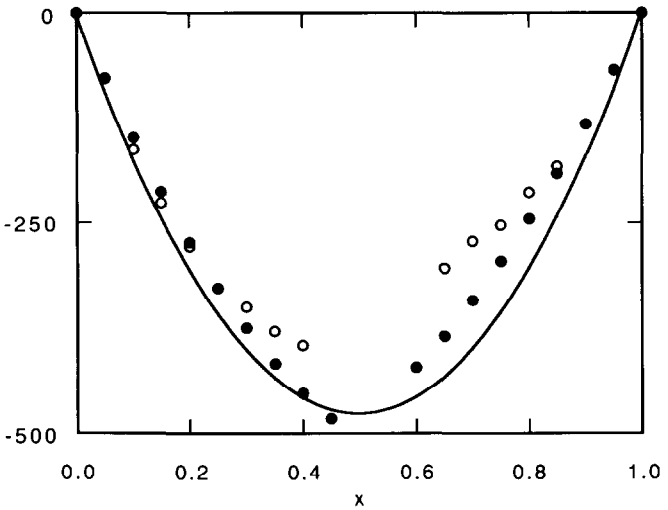

Fig. 5. G^E and H_m in J mol^{-1} [10] of the $LiNO_3$–$NaNO_3$ system plotted against the mole fraction of $NaNO_3$; ○, experimental values; ●, adjusted values for the first of expressions (19); solid line, values of H_m.

Hersh [10], are respectively

$$\left.\begin{aligned} G^E &= (-18910 - 27.51T \ln T + 205.27T)x(1-x) \\ G^E &= (-5310 - 6.008T \ln T + 30.50T)x(1-x) \end{aligned}\right\} \quad (19)$$

They are represented in Figs. 5 and 6 together with the experimental values. From these plots we may conclude that expressions (17) and (18) constitute a good approximation of regular behaviour for mixtures along the liquid curve, especially for the $LiNO_3$–KNO_3 system.

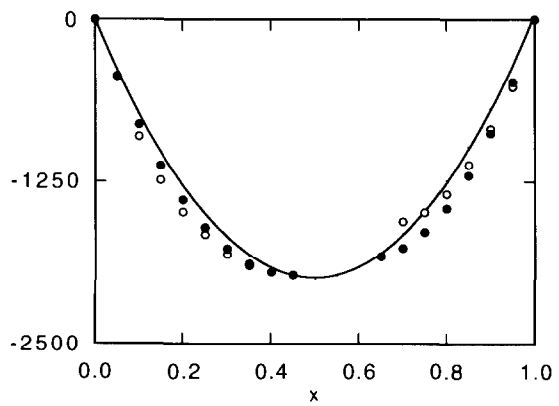

Fig. 6. G^E and H_m in J mol^{-1} [10] of the $LiNO_3$–KNO_3 system plotted against the mole fraction of KNO_3; ○, experimental values; ●, adjusted values for the first of expressions (19); solid line, values of H_m.

REFERENCES

1 P.L. Lin, A.D. Pelton and C.W. Bale, J. Am. Ceram. Soc., 62(7, 8) (1979) 414.
2 L. Kaufman, Computer Calculations of Phase Diagrams, Academic Press, New York, 1970.
3 C. Sinistri and P. Franzosini, Ric. Sci. Parte 2 Sez. A, 33 (1963) 419.
4 C. Vallet, J. Chem. Thermodyn., 4 (1972) 105.
5 C.M. Kramer and C.J. Wilson, Thermochim. Acta, 42 (1980) 253.
6 H.A.J. Oonk, Phase Theory. The Thermodynamics of Heterogeneous Equilibria, Elsevier, Amsterdam, 1981.
7 M. Hillert, Thermochim. Acta, 129 (1988) 71.
8 J. Richter and S. Sehm, Z. Naturforsch, Teil A, 27 (1972) 141.
9 M.J. Maeso, Tesis Doctoral, Universidad de Cantabria, Spain, 1992.
10 O.J. Kleppa and L.S. Hersh, J. Chem. Phys., 36(2) (1962) 544.